Antarctic Science 20 (1), 89–98 (2008) © Antarctic Science Ltd 2008 Printed in the UK DOI: 10.1017/S095410200700079X

Dating late Cenozoic erosional surfaces in Victoria Land, Antarctica, with cosmogenic neon in pyroxenes

P. OBERHOLZER[1]*, C. BARONI[2], M.C. SALVATORE[3], H. BAUR[1] and R. WIELER[1]

[1]*Institute of Isotope Geology and Mineral Resources, ETH Zürich, Clausiusstrasse 25, 8092 Zürich, Switzerland*
[2]*Dipartimento di Scienze della Terra, Università di Pisa, Via S. Maria 53, 56126 Pisa, Italy*
[3]*Dipartimento di Scienze della Terra, Università di Roma "La Sapienza", Piazzale A. Moro 5, 00185 Roma, Italy*
**current address: Baugeologie und Geo-Bau-Labor Chur, Bolettastrasse 1, 7000 Chur, Switzerland*
peter.oberholzer@tele2.ch

Abstract: We present ^{21}Ne exposure ages of erosional glaciogenic rock surfaces on nunataks in northern Victoria Land, Antarctica: i) in the Prince Albert Mountains and ii) near Mesa Range. These nunataks are located directly at the margin of the polar plateau and therefore provide an immediate record of ice volume changes of the East Antarctic Ice Sheet, not biased by ice shelf grounding or narrow valley sections downstream the outlet glaciers. The sampling locations overlook the present ice surface by less than 200 m, but were last covered by ice 3.5 Ma BP (minimum age, not corrected for erosion). This strongly indicates that the ice sheet has not been substantially thicker than today since at least the early Pliocene, which supports the hypothesis of a stable East Antarctic Ice Sheet. First absolute ages are reported for the alpine topography above the erosive trimline that typically marks the upper limit of glacial activity in northern Victoria Land. Unexpectedly low nuclide concentrations suggest that erosion rates on the alpine topography are considerably higher due to the steep slopes than those affecting flat erosional surfaces carrying Antarctic tors.

Received 29 November 2006, accepted 28 May 2007

Key words: Antarctic tors, East Antarctic Ice Sheet, Mesa Range, noble gases, Prince Albert Mountains, surface exposure dating

Introduction

The discussion around the history of the East Antarctic Ice Sheet (EAIS) has for decades been dominated by the debate between "dynamists" and "stabilists". The dynamic ice sheet hypothesis proposes that the EAIS volume was strongly reduced several times in the past 14 Ma, following climate fluctuations, including an ice sheet collapse in early Pliocene and subsequently renewed build-up of ice (Webb *et al.* 1984, Webb & Harwood 1991). The stabilists, on the other hand, state that the EAIS did not vary much in size for at least the past 15 Ma, as the Antarctic climate was constantly cold and hyperarid (Denton *et al.* 1991, Marchant *et al.* 1993, Schäfer *et al.* 2000). Many key arguments in this debate are based on evidence from the McMurdo Dry Valleys, as they contain one of the largest ice-free areas of the continent with well-preserved glacial landforms. Van der Wateren *et al.* (1999), using tectonic arguments, insist that landscape stability as inferred from evidence from the Dry Valleys cannot be generalized for the entire Transantarctic Mountains (TAM). To test this point, and to further improve our knowledge about ice volume fluctuations of the EAIS - in both a temporal and a spatial sense - we have investigated areas outside the McMurdo Dry Valleys.

Ice-free terrain is abundant north of the Dry Valleys, occurring in mountain ranges and as nunataks at the edge of the vast inland ice. Some of these nunataks protrude from the present-day ice surface by less than 200 m on the stoss side, but up to 1000 m on the lee side relative to present-day ice flow directions. Their vicinity to the EAIS makes the nunataks at the poleward side of the TAM excellent archives for the history of inland ice volume variations. Glaciogenic landforms such as erosional trimlines and alpine topography on these nunataks are a direct record of ice elevation variations. This is because the ice level around them is not influenced by the damming effects of narrow valley sections or of a grounded Ross Ice Shelf at the valley heads, as is the case for the large outlet glaciers that drain the ice sheet through the TAM. Furthermore, reconstructions of the inland ice level based on evidence from the periphery of the ice sheet do not depend upon backward extrapolations of former glacier profiles (Marchant *et al.* 1994, Denton & Hughes 2000).

We investigated glacial erosional surfaces in two areas of Victoria Land: in the Prince Albert Mountains south of David Glacier (Ford Peak, Mount Bowen) and in the Mesa Range region south of Rennick Glacier (Chisholm Hills), about 250 km and 450 km north of the Dry Valleys, respectively (Fig. 1).

Glacial geological and geomorphological setting

The geomorphology of the area is strongly controlled by the geological structure. An erosion surface (known in

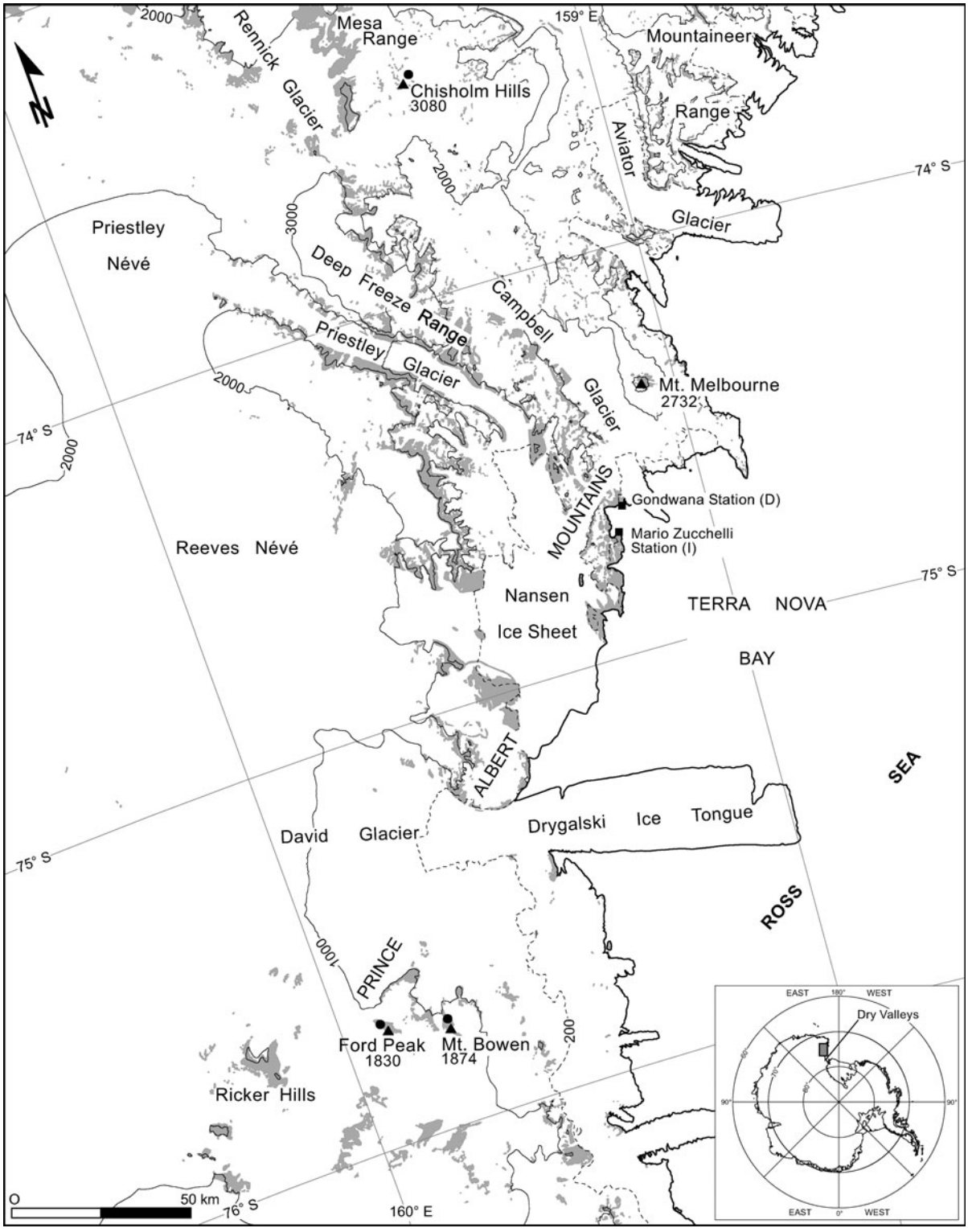

Fig. 1. Index map of the Terra Nova Bay area with sampling sites (points). Contour lines (elevation in metres) and ice free areas (grey patches) are redrawn from Antarctic Digital Database 4.0 (British Antarctic Survey 2002).

southern Victoria Land as Kukri Peneplain, Isbell 1999) sculptured in the basement carries the continental Beacon Sandstone (Triassic; McKelvey *et al.* 1977) that was later intruded by the Ferrar Dolerite (Jurassic; Harrington 1958), which built horizontal sills along the basal Beacon horizon. Flat surfaces related to the exhumation

https://doi.org/10.1017/S095410200700079X Published online by Cambridge University Press

of the Kukri Peneplain are visible on the Southern Cross Mountains whereas structural flat surfaces on top of doleritic intrusions are more widespread (from the McMurdo Dry Valleys northern margin to the Rennick Glacier area, at the internal margin of the TAM). These flat structural surfaces are to be found on several nunataks at the margin of the EAIS. Columnar jointing is a common feature along the cliffs where dolerites and basalts crop out.

The landforms of glacial origin in northern Victoria Land are described in detail in Denton *et al.* (1986), Orombelli (1989), Orombelli *et al.* (1991), and Baroni *et al.* (2005c). First absolute datings have been accomplished by Armienti & Baroni (1999) who provided K–Ar and Rb–Sr ages of igneous rocks from different landscape elements. Particular features are glacial trimlines that mark the upper limit of the erosional activity of ice, and sharp ridges with serrated spires above the uppermost trimlines, untouched by the ice (arétés). The latter landform is a very distinct feature of relict "alpine topography", which is further characterized by spurs, horns, U-shaped valleys, and cirques (Orombelli *et al.* 1991). It occurs both in granite and dolerite surfaces and is widespread in northern Victoria Land. The rock surfaces display an oxidation crust or weathering rind and are often affected by cavernous weathering. The lower limit of the sharp ridges and spires is in places obvious as the above mentioned distinct trimline that marks the upper limit of direct glacial action. At the valley heads, it reaches down to the present-day ice level. Orombelli *et al.* (1991) and Baroni *et al.* (2005a, 2005b, 2005c) give a detailed description of the distribution of the trimline between the Mesa Range and David Glacier. It is assumed that the development of the alpine topography began with the onset of glaciation on a previously sculpted fluvial valley network through undercutting of rock walls after 34 Ma BP (Sugden & Denton 2004, Jamieson *et al.* 2005, Baroni *et al.* 2005d), and that the alpine topography is the oldest landscape element in Victoria Land.

Below the trimline, sedimentary and erosional landscape elements of glacial origin are abundant in Victoria Land. According to Sugden & Denton (2004), the activity of temperate glaciers in sculpting the alpine morphology endured since about 14 Ma BP, whereas under the glacial system of northern Victoria Land, this morphology ceased to develop at 8.2 to 7.5 Ma BP (Armienti & Baroni 1999).

Landscape dynamics in northern Victoria Land today is mostly limited to periglacial processes. These processes are not efficient enough to erase the characteristics of the relict landscapes described above, such as spires or sharp ridges. In flat areas, weathering is most efficient along joints, which is best illustrated by both the formation and preservation of column-shaped erosional features called "gargoyles".

Table I. Coordinates and elevations of sampling sites.

Sample	Coordinates	Elevation (m a.s.l.)
BOW1	161°03'50"E 75°44'52"S	1700
BOW2	161°03'50"E 75°44'52"S	1700
BOW3	161°03'50"E 75°44'52"S	1700
BOW4	161°02'11"E 75°44'37"S	1525
BOW6	161°02'11"E 75°44'37"S	1525
CH2	163°13'30"E 73°29'04"S	2790
CH3	163°13'30"E 73°29'04"S	2790
CH4	163°27'29"E 73°27'02"S	2700
CH5	163°27'29"E 73°27'02"S	2700
FOR2	160°27'54"E 75°43'15"S	1800
FOR4	160°27'54"E 75°43'15"S	1800

Sampling sites

Coordinates and elevation of sampling sites are given in Table I.

David Glacier area - Mount Bowen

Mount Bowen is a nunatak 50 km inland from the Ross Sea coast, very near to the inland ice plateau. It is 6 km long and 3 km wide. As the ice flows around Mount Bowen in a generally north-easterly direction, its surface drops from 1400 to 800 m a.s.l. This abrupt topographic step locally increases the prevailing strong katabatic winds, which leads to high ice ablation rates and blue-ice surfaces in the lee of the nunatak and locally reverses the ice flow direction. The sampled "gargoyles" are found in a field of several hundred square metres at 1525 m a.s.l., clearly below the oldest erosional trimline that appears a few kilometres away at 1750 m a.s.l.

In addition to the "gargoyles", we sampled a small bench 50 m below the oldest trimline, at 1700 m a.s.l. Flat dolerite

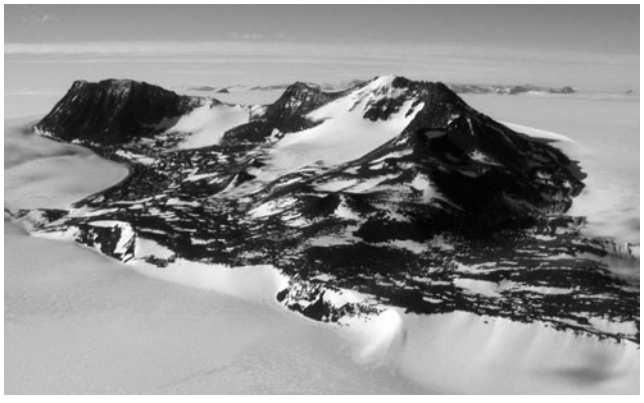

Fig. 2. Ford Peak, view from the north-east. General ice flow direction is from the back to the front of the photograph. The ice level drops by roughly 300 m from the stoss side to the lee side of the nunatak.

https://doi.org/10.1017/S095410200700079X Published online by Cambridge University Press

Fig. 3. Antarctic tors or "gargoyles" on Chisholm Hills. These tors are smaller than those on Mount Bowen, reaching heights of about 50 cm.

Fig. 4. Antarctic tors or "gargoyles" on Mount Bowen. The column in the picture is approximately 1 m high (note hammer on top of the column).

tables of more than one square metre are covered with the same stain coat and desert varnish, but glacial striae are preserved as well. These striae indicate ice flow in north-easterly direction towards David Glacier. This is consistent with the flow pattern observed on nearby Ricker Hills.

David Glacier area - Ford Peak

Ford Peak lies about 18 km north-west of Mount Bowen and has about the same size (Fig. 2). The crests of the mountain display alpine topography with indented ridges and numerous spires. Immediately below the spires, "gargoyles" are locally preserved.

We sampled the tops of single dolerite spires on an exposed crest at 1800 m a.s.l. These spires are rubefied, oxidised and affected by pithole and Tafoni weathering.

Chisholm Hills (Mesa Range)

Situated at the southern end of Mesa Range, Chisholm Hills is a group of small nunataks, 90 km from the Ross Sea coast and over 260 km north of the two sampling sites described above. Like those, the Chisholm Hills are located at the inner side of the TAM, roughly at the elevation of the local inland ice surface. On Chisholm Hills, samples were collected at two locations:

a) At the foot of a steep, sharp and serrated ridge in deeply weathered dolerite rock, sculpted by alpine topography (2790 m a.s.l.). This ridge is entirely surrounded by ice. The trimline is visible at the base of the spires, but is locally covered by accumulated snow at the foot of the ridge. These samples were collected from deeply cracked and partially loose bedrock, in awareness of the possibility that the condition of the rock may lead to a strong underestimation of the surface exposure age (see discussion section).

b) On a small flat dolerite bench entirely covered with "gargoyles" (2700 m a.s.l., Fig. 3). This terrace is at a lower elevation than the serrated ridge, thus, the situation is comparable to that at Mount Bowen and Ford Peak, where the "gargoyles" characterize flat surfaces below the trimline and thus below the alpine topography. The "gargoyles" at Chisholm Hills are in general shorter and narrower than those at Mount Bowen, reaching heights of 70 cm.

Methods

Geomorphological survey and landscape analysis

The main landscape features of the region were surveyed by helicopter traverse and detailed geomorphological surveys in key areas in the period 1986–2004. Results are presented and discussed in Orombelli *et al.* (1991), Armienti & Baroni (1999), and Baroni *et al.* (2005a, 2005d). Landscape analysis was conducted over an area extending more than 300 km along the coastal margin and several tens of km into the interior, enabling us to distinguish several relict geomorphologic features, dominated by an alpine topography that is widespread in entire Victoria Land.

Glacial erosional trimlines were identified and their elevations mapped using topographic maps and altimeter

https://doi.org/10.1017/S095410200700079X Published online by Cambridge University Press

Table II. Neon isotope data for all samples[1].

Sample	T (°C), time (min)	^{20}Ne (10^9 at g^{-1})	$^{21}Ne/^{20}Ne$ (10^{-3})	$^{22}Ne/^{20}Ne$	$^{21}Ne_{exc}$ (10^5 at g^{-1})
BOW1	850, 45	13.07 ± 0.17	7.45 ± 0.13	0.1066 ± 0.0016	590 ± 30
	1500, 15	1.77 ± 0.04	18.87 ± 0.73	0.1163 ± 0.0029	280 ± 20
	1750, 15	*1.95 ± 0.06*	*2.86 ± 0.32*	*0.1008 ± 0.0034*	*0*
Total					870 ± 50
BOW2	850, 45	10.43 ± 0.17	6.30 ± 0.23	0.1055 ± 0.0010	350 ± 30
	1500, 15	4.05 ± 0.10	8.46 ± 0.31	0.1047 ± 0.0056	220 ± 20
	1750, 15	*6.94 ± 0.25*	*2.96 ± 0.16*	*0.1028 ± 0.0033*	*0*
Total					570 ± 50
BOW3	850, 45	11.00 ± 0.15	5.76 ± 0.15	0.1055 ± 0.0019	310 ± 20
	1500, 15	3.42 ± 0.03	17.04 ± 0.19	0.1175 ± 0.0039	480 ± 10
	1750, 15	*5.61 ± 0.10*	*3.00 ± 0.11*	*0.1028 ± 0.0016*	*0*
Total					790 ± 30
BOW3-2	850, 45	10.10 ± 0.17	6.30 ± 0.24	0.1087 ± 0.0020	330 ± 30
	1500, 15	1.45 ± 0.04	35.51 ± 0.79	0.1360 ± 0.0042	470 ± 20
	1750, 15	*1.23 ± 0.02*	*2.98 ± 0.31*	*0.1002 ± 0.0030*	*0*
Total					800 ± 50
BOW4	850, 45	14.04 ± 0.07	18.18 ± 0.37	0.1194 ± 0.0013	2140 ± 70
	1500, 15	2.97 ± 0.10	58.71 ± 1.58	0.1681 ± 0.0105	1660 ± 80
	1750, 15	*2.47 ± 0.07*	*3.64 ± 0.19*	*0.1023 ± 0.0023*	*20 ± 10*
Total					3820 ± 160
BOW6	850, 45	49.75 ± 0.18	7.52 ± 0.05	0.1074 ± 0.0004	2270 ± 60
	1500, 15	2.78 ± 0.11	41.13 ± 1.28	0.1548 ± 0.0076	1060 ± 60
	1750, 15	*2.28 ± 0.08*	*3.20 ± 0.22*	*0.1016 ± 0.0023*	*10 ± 10*
Total					3340 ± 130
CH2	850, 45	25.57 ± 0.21	4.46 ± 0.06	0.1043 ± 0.0005	390 ± 30
	1500, 15	1.66 ± 0.04	8.74 ± 0.42	0.1096 ± 0.0037	100 ± 10
	1750, 15	*1.18 ± 0.05*	*2.97 ± 0.30*	*0.1001 ± 0.0041*	*0*
Total					490 ± 40
CH3	850, 45	81.04 ± 0.43	3.27 ± 0.04	0.1024 ± 0.0004	250 ± 50
	1500, 15	*1.53 ± 0.07*	*3.98 ± 0.38*	*0.0986 ± 0.0020*	*20 ± 10*
	1750, 15	*1.82 ± 0.02*	*3.08 ± 0.24*	*0.1000 ± 0.0041*	*0*
Total					270 ± 60
CH4	850, 45	2.91 ± 0.08	68.32 ± 1.96	0.1704 ± 0.0056	1900 ± 90
	1400, 15	2.63 ± 0.07	200.16 ± 3.30	0.3150 ± 0.0077	5190 ± 200
	1750, 15	*2.53 ± 0.06*	*3.17 ± 0.10*	*0.1020 ± 0.0018*	*0*
Total					7090 ± 290
CH5	850, 45	4.68 ± 0.08	29.19 ± 1.02	0.1299 ± 0.0046	1230 ± 60
	1400, 15	2.80 ± 0.08	126.12 ± 2.49	0.2356 ± 0.0098	3450 ± 140
	1750, 15	*4.90 ± 0.09*	*3.16 ± 0.08*	*0.1020 ± 0.0019*	*10 ± 10*
Total					4690 ± 210
FOR2	*850, 45*	*3.16 ± 0.08*	*7.83 ± 0.39*	*0.1054 ± 0.0015*	*150 ± 20*
	1400, 15	3.18 ± 0.09	78.11 ± 1.97	0.1830 ± 0.0069	2400 ± 110
	1750, 15	*2.13 ± 0.12*	*3.06 ± 0.16*	*0.1015 ± 0.0021*	*0*
Total					2550 ± 130
FOR4	850, 45	3.74 ± 0.07	6.76 ± 0.16	0.1057 ± 0.0024	140 ± 10
	1500, 15	3.19 ± 0.07	60.40 ± 1.47	0.1641 ± 0.0069	1830 ± 70
	1750, 15	*2.49 ± 0.09*	*3.15 ± 0.19*	*0.1025 ± 0.0017*	*0*
Total					1970 ± 80

[1] Errors are 2σ and include uncertainties in mass discrimination and sensitivity; uncertainties of calibration gas concentrations are not included, but expected to be smaller than 3%. $^{21}Ne_{exc}$ is assumed to be entirely cosmogenic. BOW3-2 is a second sample from the same surface as BOW3. Temperature steps in *italic* were not used for age calculation (see text).

measurements, corrected by cross-checking points of known elevation (Baroni *et al.* 2005a, 2005b, 2005c). The estimated trimline elevations have an uncertainty of about 50 m.

Sampling

Seven samples were taken from erosional surfaces, four of them from a particular weathering feature that commonly is referred to as "Antarctic Tors" (Selby 1972) or with the more evocative term of "gargoyles" (Pocknall *et al.* 1994) (Figs 3 & 4). These are columns of Ferrar Dolerite, preferably of more fine-grained, resistant lithology, weathered to pitted towers up to two metres in height and reminiscent of "gargoyles", statues at waterspouts in medieval architecture. Most columns are 60–80 cm high, with diameters from 10–40 cm. They occur in groups of

https://doi.org/10.1017/S095410200700079X Published online by Cambridge University Press

several dozens, standing at most a few metres apart. Common features are excessive pithole-weathering on the top surface (diameters of weathering pits are 1–5 cm) and a strong weathering rind with an often shiny desert varnish on the top surfaces, resembling the surface properties of the alpine topography. "Gargoyles" occur in groups on flat terraces that are thought to be structurally controlled, i.e. to coincide with the original surface of the dolerite intrusion. It is assumed that "gargoyles" have developed between intersecting cooling cracks, similar to basalt columns. Thus, their top surfaces are assumed to be the oldest remnants of the original continuous rock surface. Erosion is assumed to be lowest on the column tops as the strong desert varnish on these surfaces is a micro sediment accreted on the external surface. Neither chemical weathering, nor exfoliation have affected the varnish since deposition, thus, the top surfaces of the "gargoyles" did not experience any erosion since varnish deposition (Giorgetti & Baroni 2007). In contrast, the effects of strong erosion are documented by the surfaces between the tors, which are considerably lower and show excessive exfoliation. To our knowledge, this study is the first attempt to directly date "gargoyles" in Antarctica.

The "gargoyles" investigated here are all found at elevations below the highest trimline. Hence, the mutual topographic position of trimline and "gargoyles" suggests that the ice that sculpted the trimline originally covered the terraces that carry the "gargoyles".

We have dated the most extensive glaciation in northern Victoria Land by determining exposure ages for the uppermost trimline. This was achieved first by dating surfaces of the alpine topography above the trimline (Ford Peak and Chisholm Hills), and second by dating erosional surfaces below the trimline (Chisholm Hills and Mount Bowen), some of them carrying "gargoyles". The latter samples are expected to yield a minimum age for the trimline. Samples were taken at locations where a trimline is directly related to earlier EAIS ice levels, avoiding trimlines created by local ice caps and mountain glaciers.

Nuclide measurements

Rock samples were crushed and sieved to a grain size of 100 to 315 µm. Pyroxene separates were produced by magnetic and heavy liquid separation and, if necessary, by hand-picking.

Both neon and helium isotopes were analysed in the pyroxene separates. Strong variations between the resulting He and Ne ages indicate that some of the analysed mineral separates contained plagioclase, which does not retain cosmogenic He (e.g. Bruno *et al.* 1997; see results section). Therefore, we preferred not to use the He data for age calculation.

Samples were degassed by stepwise heating in an electron impact furnace. The temperature steps were chosen at 850°C to check for possible trapped or nucleogenic ^{21}Ne, at 1400 or 1500°C for cosmogenic ^{21}Ne and at 1750°C for total extraction, following Schäfer *et al.* (2000) (Table II). The sample gas was cleaned with Zr–Ti and *SAES* non-evaporable getters and nitrogen-cooled cold traps. Nuclide concentrations were measured with a non-commercial 90° sector field noble gas mass spectrometer equipped with a modified Baur-Signer ion source and a molecular drag pump which pumps He and Ne almost quantitatively into the ionization volume, thus increasing the sensitivity of the spectrometer by two orders of magnitude (Baur 1999). The electron acceleration voltage in the ion source was set to 45 V to suppress double chargings of ^{40}Ar and $^{44}CO_2$. Interferences of $H_2^{18}O$ (0.2% of the total H_2O) and

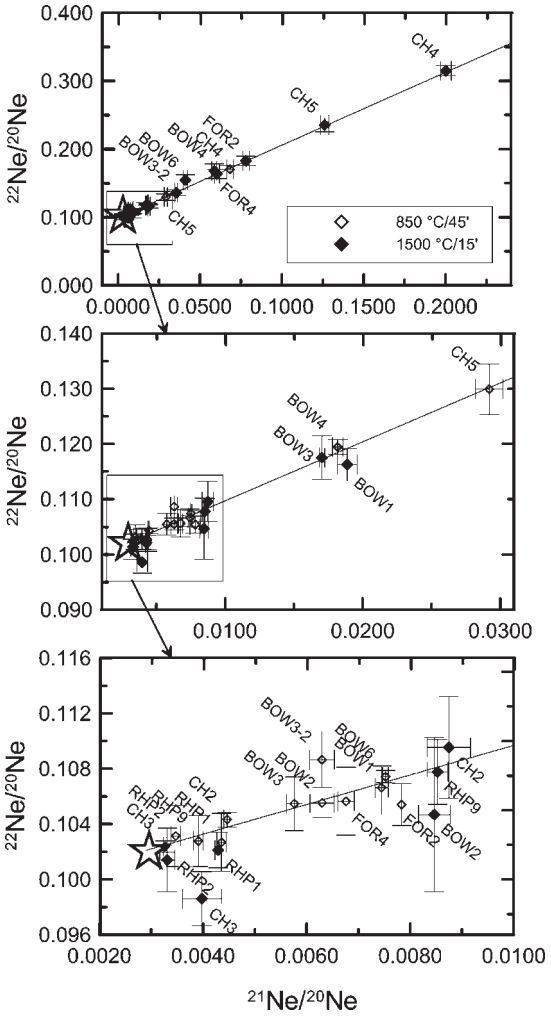

Fig. 5. Three isotope plot of the neon data from pyroxene. Open diamonds are 850°C steps, and filled diamonds are 1400/1500°C steps. 1750°C steps are omitted as they are of atmospheric composition within errors. The star symbol in each panel represents atmospheric composition (2.959×10^{-3} / 0.102, Eberhardt *et al.* 1965). The atmospheric / cosmogenic mixing line is drawn as $y = 1.069\ x + 0.099$ (Schäfer *et al.* 1999).

https://doi.org/10.1017/S095410200700079X Published online by Cambridge University Press

Table III. Relative concentrations of the elements that produce $^{21}Ne_{cos}$, and ^{21}Ne production rates.

Sample	Si (weight %)	Mg (weight %)	Al (weight %)	P_{21} slhl[1] (at/g/yr)	P_{21} scaled[2] (at/g/yr)
BOW1	28.8	2.6	6.8	20.5	118.3
BOW2	27.6	2.6	3.6	18.3	105.6
BOW3	27.4	11.2	4.2	34.6	199.6
BOW4	24.9	6.6	3.0	24.2	121.9
BOW6	25.7	4.3	2.9	20.3	102.3
CH2	26.7	1.9	7.6	18.7	196
CH3	38.3	0.1	3.9	18.3	203.5
CH4	24.9	10.4	1.1	30.4	228.8
CH5	24.6	10.1	1.7	30.1	223.9
FOR2	24.7	11.0	1.0	31.5	351.5
FOR4	25.1	11.7	0.9	32.7	348

[1] ^{21}Ne production rate at sea level and high latitude (slhl), calculated with $P_{21}(Si) = 42.5$ at/g/yr, $P_{21}(Mg) = 185$ at/g/yr, and $P_{21}(Al) = 51$ at/g/yr (Schäfer *et al.* 2000)
[2] ^{21}Ne production rate at sampling location, scaled according to Stone (2000).
Uncertainties of the concentrations are below 1% for Mg and Si and below 4% for Al

remaining $^{40}Ar^{++}$ (0.045% of the total ^{40}Ar) on mass 20 were corrected for, corresponding typically to a correction of the ^{20}Ne signal of 0.1%. Interferences of remaining $^{44}CO_2^{++}$ were negligible.

Age calculation

Cosmogenic neon ($^{21}Ne_{cos}$) was calculated as the excess over air, assuming that no nucleogenic is present even in the 850°C steps, as indicated by the three-isotope-plot (Fig. 5). We used elemental ^{21}Ne production rates of 42.5 at/g/yr (Si), 185 at/g/yr (Mg), and 51 at/g/yr (Al) (Niedermann 2000, Schäfer *et al.* 2000). The concentrations of these elements were determined by ICP-OES and atomic absorption spectroscopy (Table III). Total production rates were scaled to the geomagnetic latitude and elevation of the sampling sites with the formalism suggested by Stone (2000), compensating for the Antarctic air pressure anomaly.

The 850 and 1400/1500°C steps were used to calculate exposure ages. The only exception is CH3, where almost all cosmogenic Ne was released at 850°C (Table II).

For samples from non-flat surfaces, some of the incoming cosmic-ray neutrons escape from the rock back to the atmosphere, reducing the effective nuclide production rate (Masarik & Wieler 2003). The distinct columnar shape of the "gargoyles" is particularly affected by this process. A correction in the range of 4 to 7% was applied according to Masarik & Wieler (2003).

Table IV. Minimum surface exposure ages and maximum erosion rates (calculated from ^{21}Ne data under the assumption of infinite exposure)[1].

Sample	surface type	geometry correction[2] (%)	Total neon age (ka)	E_{max} (^{21}Ne) (cm Ma^{-1})
BOW1	sb	0	733 ± 39	76 ± 4
BOW2	sb	0	541 ± 49	103 ± 9
BOW3	sb	0	396 ± 19	140 ± 7
BOW4	T	7	3331 ± 136	18 ± 1
BOW6	T	7	3485 ± 126	17 ± 1
CH2	*at*	*0*	*210 ± 16*	*264 ± 20*
CH3	*at*	*0*	*111 ± 21*	*500 ± 93*
CH4	T	4	2098 ± 85	28 ± 1
CH5	T	5	1412 ± 60	41 ± 2
FOR2	at	0	1299 ± 63	43 ± 2
FOR4	at	0	971 ± 42	57 ± 2

[1] Surface types: sb = striated bedrock, T = Antarctic Tor, at = alpine topography. Parameters used for calculations: density $\rho = 2.7$ g cm^{-3}, attenuation length $L = 150$ g cm^{-2}). Ages include geometry correction. Samples in *italic* were not used for age discussion (see text).
[2] Correction for neutron escape from non-flat surfaces after Masarik & Wieler (2003).

Results

Detailed results are shown in Tables II–IV and Fig. 5.

As indicated by considerable variations between the He and Ne ages, the procedure described above for separating pyroxene crystals from the very fine-grained dolerite rocks was not efficient enough. The difficulty of separating pyroxene and feldspar in Ferrar Dolerite has been observed before by Bruno *et al.* (1997) and Niedermann *et al.* (2007). From seven out of eleven samples, no material was left to determine the mineral composition quantitatively. Qualitative X-ray diffractometry (XRD) analysis of the other four samples confirmed that they contained significant fractions of plagioclase (Ferrar Dolerite contains up to 60% of plagioclase).

Bruno *et al.* (1997) found, by comparison of pyroxene and whole rock aliquots, that plagioclase in their Ferrar Dolerite samples lost about half of its cosmogenic ^{21}Ne. Therefore, the most probable result of plagioclase contamination in pyroxene samples is an underestimation of exposure ages due to the loss of ^{21}Ne from plagioclase, which acts in the same direction as unaccounted-for erosion, emphasizing that all ages reported here are strict minimum ages.

Samples CH2 and CH3 are left out from the discussion of exposure ages. Originating from the alpine topography, they are expected to be contemporary to or older than CH4 and CH5 from below the trimline. However, CH2 and CH3 show hardly any ^{21}Ne excess. This is not surprising, as thick slabs of rock detached from the sampled surfaces indicate very high local erosion rates. Therefore, CH2 and CH3 are not considered for the discussion of the exposure ages.

Discussion

The surface exposure ages reported here have to be regarded as strict minimum ages as they do not take into account the effects of erosion, temporary shielding and plagioclase contamination. Therefore, for discussion we consider the highest minimum age of a landform to be a reliable lower

https://doi.org/10.1017/S095410200700079X Published online by Cambridge University Press

limit for the duration for which that landform has been ice-free.

The point in time when erosive ice sculpted the terraces today covered with "gargoyles", engraved the trimline and initiated the development of the alpine topography above, is best approximated by the highest minimum age obtained in this study, which is 3.5 Ma, determined on a "gargoyle" at Mount Bowen in the David Glacier area. The corresponding age for the Mesa Range (Chisholm Hills) is 2.1 Ma. This age difference is interpreted to be largely the result of a different degree of plagioclase contamination. It is not likely to represent a difference in the timing of ice retreat.

From these ages and from the position of the sampling sites, we infer that the ice of the outermost domes of the EAIS has not attained the elevation of the gargoyle terraces anymore after 3.5 Ma BP, which implies minimal variations of the ice surface level since at least Mid-Pliocene. An immediate constraint on how small the maximum ice level variation was is obtained from the "gargoyles" on Chisholm Hills. The terrace where the samples were collected overlooks the ice by no more than 250 m today. That is, the surface elevation of the EAIS has never been more than 250 m higher than today since at least 2.1 Ma BP, or rather since more than 3.5 Ma BP, as suggested by the Mount Bowen samples. On Mount Bowen, the maximum elevation change is less obvious, as the "gargoyles" are located at a lower elevation than the adjacent present-day ice sheet surface. Local ice flow patterns are ruled by the sub-ice bedrock topography and the strong katabatic winds, producing an ice surface with a high relief around Mount Bowen. Observations on the present-day ice surface suggest that the inland ice is likely to overflow the terrace with "gargoyles" if its surface elevation at the stoss-side of the nunatak is more than about 200 m higher than today.

The sampled surfaces on the higher platform on Mount Bowen (samples BOW1 to BOW3) are located 175 m higher than the tors, but still below the trimline. Their exposure ages range from 396 to 733 kyr, considerably younger than the "gargoyles". Erosion must be ruled out as a reason for these young apparent ages, as glacial striae were preserved on the analysed surfaces. A more likely explanation again comes from the local ice flow patterns. It seems reasonable that, at times of a slightly elevated inland ice level, the ice may well cover the terrace at 1700 m a.s.l. near the summit of the nunatak, whereas the "gargoyles", situated a few kilometres downstreams at 1525 m a.s.l., remain ice-free.

The alpine topography is the second landscape element dated in this study. It is expected to be older than the underlying trimline and the "gargoyles". However, the nominally oldest alpine topography sample, FOR2 from Ford Peak, yielded a minimum age of only 1.3 Ma. This is interpreted to reflect strong erosion of the very steep relief above the trimline. Periglacial processes are enhanced on strongly inclined surfaces such as the slopes of the alpine topography, where the development of a protecting debris cover is prevented. This is particularly obvious at the sampling site of the omitted samples from Chisholm Hills (CH2 and CH3), where it was not possible to determine a surface exposure age due to spalling rock surfaces (see results section). The lower $^{21}Ne_{cos}$ concentrations in the Ford Peak samples thus are a consequence of high erosion rates, and not of short exposure time.

Maximum erosion rates, calculated under the assumption of infinite exposure time, are 34 and 57 cm Ma^{-1} for the alpine topography, and between 17 and 41 cm Ma^{-1} for the "gargoyles" (Table IV). These numbers are similar to those determined for granite bedrock near Terra Nova Bay (Oberholzer *et al.* 2003) or for Beacon Sandstone in the Dry Valleys (Nishiizumi *et al.* 1991). The true erosion rates are likely to be even lower than the values given in Table IV. These low rates testify for constantly cold and exceedingly dry climatic conditions prevailing in Antarctica since at least early Pliocene.

Conclusions

Two types of ancient erosional rock surfaces from the northern and the southern part of northern Victoria Land were dated for the first time: dolerite rock columns referred to as Antarctic tors, or "gargoyles", and the alpine topography, a type of morphology with serrated ridges and steep rock walls, widespread above the highest and oldest trimline in northern Victoria Land, and thus regarded as the oldest landscape feature preserved. The resulting minimum exposure ages are 2.1–3.5 Ma for the "gargoyles" and only 1.3 Ma for the alpine topography. This "age reversal" is due to more severe erosion on the alpine topography.

From these ages and the position of the sampling sites it is inferred that the surface elevation of the EAIS and its outlet glaciers in northern Victoria Land has not exceeded the modern level by more than 200 to 250 m for at least 3.5 Ma. Correction for erosion would increase this time range. Maximum erosion rates were as low as 16 cm Ma^{-1} on the "gargoyles" terraces. On the alpine topography, they are two to three times higher due to the steep relief and the associated enhancement of periglacial processes.

Such small variations in surface elevation of the EAIS in two regions of northern Victoria Land, as inferred from the data presented here, agree well with corresponding glacial geological evidence from the McMurdo Dry Valleys and the Terra Nova Bay area (Denton *et al.* 1991, Marchant *et al.* 1994, Oberholzer *et al.* 2003) that testifies for very restricted dynamics of the EAIS. Hence, ancient glacial landscapes are not unique to the well-studied Dry Valleys, but also occur in northern Victoria Land. This extends the concept of long-term landscape stability beyond southern Victoria Land; persistent climate stability with cold and

arid conditions seems to be a feature of large parts of the TAM, having left landscapes unchanged since at least early Pliocene. This contradicts the hypothesis which explains the antiquity of the Dry Valleys' landscapes with differences in uplift between tectonic blocks of the TAM (Van der Wateren *et al.* 1999). Thus, our dataset contributes to the large body of evidence in support of a stable behaviour of the EAIS since at least early Pliocene.

However, more information on the history of ice level variations in both southern and northern Victoria Land is required in order to correlate events of ice advance and retreat in those areas and confirm the over-regional character of glacial chronologies.

Acknowledgements

This work was supported by the Italian Programme on Antarctic Research (PNRA) and the Swiss National Science Foundation. Francesco Fasano was a great help with the collection of the samples. Stefan Strasky and Manuel Eggimann helped investigating the mineralogical composition of the samples. We appreciate the comments by S. Niedermann and an anonymous reviewer which greatly improved the manuscript.

References

Armienti, P. & Baroni, C. 1999. Cenozoic climatic change in Antarctica recorded by volcanic activity and landscape evolution. *Geology*, **27**, 617–620.

Baroni, C., Biasini, A., Bondesan, A., Denton, G.H., Frezzotti, M., Grigioni, P., Meneghel, M., Orombelli, G., Salvatore, M.C., Della Vedova, A.M. & Vittuari, L. 2005a. Mount Melbourne Quadrangle, Victoria Land, Antarctica 1:250,000 (Antarctic Geomorphological and Glaciological Map Series). *In* Haeberli, W., Zemp, M., Hoelzle, M. & Frauenfelder, R., *eds. Fluctuations of glaciers, 1995–2000* (**Vol. VIII**). Zürich: IAHS (ICSI)-UNEP-UNESCO, 38–40.

Baroni, C., Biasini, A., Cimbelli, A., Frezzotti, M., Orombelli, G., Salvatore, M.C., Tabacco, I. & Vittuari, L. 2005b. Relief Inlet Quadrangle, Victoria Land, Antarctica 1:250,000 (Antarctic Geomorphological and Glaciological Map Series). *In* Haeberli, W., Zemp, M., Hoelzle, M. & Frauenfelder, R., *eds. Fluctuations of glaciers 1995–2000* (Vol. VIII). Zürich: IAHS (ICSI)-UNEP-UNESCO, 43–44.

Baroni, C., Frezzotti, M., Salvatore, M.C., Meneghel, M., Tabacco, I.E., Vittuari, L., Bondesan, A., Biasini, A., Cimbelli, A. & Orombelli, G. 2005c. Antarctic geomorphological and glaciological 1:250,000 map series. Mount Murchison Quadrangle (northern Victoria Land). Explanatory notes. (with geomorphological map at the scale of 1:250,000). *Annals of Glaciology*, **39**, 256–264.

Baroni, C., Noti, V., Ciccacci, S., Righini, G. & Salvatore, M.C. 2005d. Fluvial origin of the valley system in northern Victoria Land (Antarctica) from quantitative geomorphic analysis. *Geological Society of America Bulletin*, **117**, 212–228.

Baur, H. 1999. A noble-gas mass spectrometer compressor source with two orders of magnitude improvement in sensitivity. *EOS Transactions AGU*, **80**, F1118

British Antarctic Survey. 2002. *Antarctic digital database, version 4.0*. Cambridge: Scientific Committee on Antarctic Research.

Bruno, L.A., Baur, H., Graf, T., Schlüchter, C., Signer, P. & Wieler, R. 1997. Dating of Sirius Group tillites in the Antarctic Dry Valleys with cosmogenic ^{3}He and ^{21}Ne. *Earth and Planetary Science Letters*, **147**, 37–54.

Denton, G.H. & Hughes, T.J. 2000. Reconstruction of the Ross Ice drainage system, Antarctica, at the Last Glacial Maximum. *Geografiska Annaler*, **82A**, 143–166.

Denton, G.H., Prentice, M.L. & Burckle, L.H. 1991. Cainozoic history of the Antarctic ice sheet. *In* Tingey, R.J., *ed. The geology of Antarctica*. Oxford: Oxford University Press, 365–433.

Denton, G.H., Bockheim, J.G., Wilson, S.C. & Schlüchter, C. 1986. Late Cenozoic history of Rennick Glacier and Talos Dome, northern Victoria Land, Antarctica. *Antarctic Research Series*, **46**, 339–375.

Eberhardt, P., Eugster, O. & Marti, K. 1965. A redetermination of the isotopic composition of atmospheric neon. *Zeitschrift für Naturforschung*, **20**, 623–624.

Giorgetti, G. & Baroni, C. 2007. High-resolution analysis of silica and sulphate-rich rock varnishes from Victoria Land (Antarctica). *European Journal of Mineralogy*, **19**, 381–389.

Harrington, H.J. 1958. The nomenclature of rock units in the Ross Sea region. *Nature*, **182**, 290.

Isbell, J.L. 1999. The Kukri Erosion Surface; a reassessment of its relationship to rocks of the beacon supergroup in the central Transantarctic Mountains, Antarctica. *Antarctic Science*, **11**, 228–238.

Jamieson, S.S.R., Hulton, N.R.J., Sugden, D.E., Payne, A.J. & Taylor, J. 2005. Cenozoic landscape evolution of the Lambert Basin, East Antarctica: the relative role of rivers and ice sheets. *Global and Planetary Change*, **45**, 35–49.

Marchant, D.R., Denton, G.H., Sugden, D.E. & Swisher, C.C. 1993. Miocene glacial stratigraphy and landscape evolution of the western Asgard Range, Antarctica. *Geografiska Annaler*, **75A**, 303–330.

Marchant, D.R., Denton, G.H., Bockheim, J.G., Wilson, S.C. & Kerr, A.R. 1994. Quaternary changes in level of the upper Taylor Glacier, Antarctica: implications for palaeoclimate and East Antarctic Ice Sheet dynamics. *Boreas*, **23**, 29–43.

Masarik, J. & Wieler, R. 2003. Production rates of cosmogenic nuclides in boulders. *Earth and Planetary Science Letters*, **216**, 201–208.

McKelvey, B.C., Webb, P.-N. & Kohn, B.P. 1977. Stratigraphy of the Taylor and Lower Victoria groups (Beacon Supergroup) between the Mackay and Boomerang Range, Antarctica. *New Zealand Journal of Geology and Geophysics*, **20**, 813–863.

Niedermann, S. 2000. The ^{21}Ne production rate in quartz revisited. *Earth and Planetary Science Letters*, **183**, 361–364.

Niedermann, S. 2002. Cosmic-ray produced noble gases in terrestrial rocks: dating tools for surface processes. *In* Porcelli, D., Ballentine, C.J. & Wieler, R., *eds. Noble gases in geochemistry and cosmochemistry*. Washington, DC: Mineralogical Society of America, 731–784.

Niedermann, S., Schaefer, J.M., Wieler, R. & Naumann, R. 2007. The production rate of cosmogenic Ar-38 from calcium in terrestrial pyroxene. *Earth and Planetary Science Letters*, **257**, 596–608.

Nishiizumi, K., Kohl, C.P., Arnold, J.R., Klein, J., Fink, D. & Middleton, R. 1991. Cosmic ray produced ^{10}Be and ^{26}Al in Antarctic rocks: exposure and erosion history. *Earth and Planetary Science Letters*, **104**, 440–454.

Oberholzer, P., Baroni, C., Schaefer, J.M., Orombelli, G., Ivy-Ochs, S., Kubik, P.W., Baur, H. & Wieler, R. 2003. Limited Pliocene/Pleistocene glaciation in Deep Freeze Range, northern Victoria Land, Antarctica, derived from *in situ* cosmogenic nuclides. *Antarctic Science*, **15**, 493–502.

Orombelli, G. 1989. Terra Nova Bay: a geographic overview. *Memorie della Società Geologica Italiana*, **32**, 69–75.

Orombelli, G., Baroni, C. & Denton, G.H. 1991. Late Cenozoic glacial history of the Terra Nova Bay region, northern Victoria Land, Antarctica. *Geografia Fisica e Dinamica Quaternaria*, **13**, 139–163.

Pocknall, D.T., Chinn, T.J., Skyes, R. & Skinner, D.N.B. 1994. *Geology of the Convoy Range area,* southern Victoria Land*,* Antarctica. Lower Hutt, New Zealand: Institute of Geological and Nuclear Sciences, 36 pp.

Schäfer, J., Baur, H., Denton, G.H., Ivy-Ochs, S., Marchant, D.R., Schlüchter, C. & Wieler, R. 2000. The oldest ice on earth in Beacon Valley, Antarctica: new evidence from surface exposure dating. *Earth and Planetary Science Letters*, **179**, 91–99.

Schäfer, J.M., Ivy-Ochs, S., Wieler, R., Leya, I., Baur, H., Denton, G.H. & Schlüchter, C. 1999. Cosmogenic noble gas studies in the oldest landscape on Earth: surface exposure ages of the Dry Valleys, Antarctica. *Earth and Planetary Science Letters*, **167**, 215–226.

Selby, M.J. 1972. Antarctic tors. *Zeitschrift für Geomorphologie*, **13**, 73–86.

Stone, J.O. 2000. Air pressure and cosmogenic isotope production. *Journal of Geophysical Research*, **105**, 23 753–23 759.

Sugden, D.E. & Denton, G.H. 2004. Cenozoic landscape evolution of the Convoy Range to Mackay Glacier area, Transantarctic Mountains: onshore to offshore synthesis. *Geological Society of America Bulletin*, **116**, 840–857.

Van Der Wateren, F.M., Dunai, T.J., Balen, R.T.V., Klas, W., Verbers, A.L.L.M., Passchier, S. & Herpers, U. 1999. Contrasting Neogene denudation histories of different structural regions in the Transantarctic Mountains rift flank constrained by cosmogenic isotope measurements. *Global and Planetary Change*, **23**, 145–172.

Webb, P.-N. & Harwood, D.M. 1991. Late Cenozoic glacial history of the Ross Embayment, Antarctica. *Quaternary Science Reviews*, **10**, 215–223.

Webb, P.N., Harwood, D.M., Mckelvey, B.C., Mercer, J.H. & Stott, L.D. 1984. Cenozoic marine sedimentation and ice volume variation on the East Antarctic craton. *Geology*, **12**, 287–291.